Journal of Renewable Materials
DOI:10.32604/jrm.2020.09615
Article

Tech Science Press

Green Composite Material Made from *Typha latifolia* Fibres Bonded with an Epoxidized Linseed Oil/Tall Oil-Based Polyamide Binder System

Günter Wuzella[1], Arunjunai Raj Mahendran[1] and Andreas Kandelbauer[2,*]

[1]Kompetenzzentrum Holz (Wood K Plus), Linz, A-4040, Austria
[2]Reutlingen University, Lehr- und Forschungszentrum Process Analysis & Technology, School of Applied Chemistry, Reutlingen, D-72762, Germany
*Corresponding Author: Andreas Kandelbauer. Email: andreas.kandelbauer@reutlingen-university.de
Received: 16 January 2020; Accepted: 20 March 2020

Abstract: Here, we report the mechanical and water sorption properties of a green composite based on *Typha latifolia* fibres. The composite was prepared either completely binder-less or bonded with 10% (w/w) of a bio-based resin which was a mixture of an epoxidized linseed oil and a tall-oil based polyamide. The flexural modulus of elasticity, the flexural strength and the water absorption of hot pressed *Typha* panels were measured and the influence of pressing time and panel density on these properties was investigated. The cure kinetics of the bio-based resin was analyzed by differential scanning calorimetry (DSC) in combination with the iso-conversional kinetic analysis method of Vyazovkin to derive the curing conditions required for achieving completely cured resin. For the binder-less *Typha* panels the best technological properties were achieved for panels with high density. By adding 10% of the binder resin the flexural strength and especially the water absorption were improved significantly.

Keywords: Natural fibre composite; Cattails; *Typha latifolia*; epoxidized linseed oil; cure kinetics; iso-conversional kinetic analysis

1 Introduction

Due to an increasing global concern for environmental sustainability, many industries currently explore the potential of natural materials to replace non-renewable resources in their processes. Many different types of vegetable fibres are becoming increasingly popular as reinforcements for composites, especially in the automotive industry [1]. Major reasons for using vegetable fibres are reduced weight, superior environmental balance, reduced costs and the possibility to manufacture complex structural elements. While there is a large scientific body of work describing the properties of fibres from plants like flax, hemp, kenaf, coco or sisal for this purpose [1,2], other plants like *Typha latifolia* are much less well known as vegetable fibre sources for reinforcing composites. *Typha* sp. grows in wetlands throughout the world and is commonly known as cattail, bulrush, or raupo. It is mainly used as an adsorbent for heavy metal elimination from contaminated fluids in phytoremediation [3–7]. *Typha* species have been used for fibre reinforced composites with polylactic acid, polyethylene and other matrix polymers [8–14].

Typha sp. show some interesting anatomical features that make them a promising plant raw material for fibre reinforcement of composites. In nature, subepidermal vascular and fibre bundles lend mechanical support against environmental stresses and additional mechanical strength is provided by ribbings and margins stemming from enlarged epidermal cells located above each fibre bundle [15]. These epidermal cells are thickly cutinized, i.e., they are covered by a continuous layer of resinous material forming a protective surface layer. The hypodermis contains suberin and especially lignin which is natural polyphenolic glue. All cells of the hypodermis have secondarily lignified cell walls [15]. The thick, lignified hypodermal zones of the roots [16] and rhizome [15] may act as a binder in composites and it has been shown that the self-gluing properties of *Typha latifolia* can be exploited for producing binder-less composites via hot pressing *Typha* fibre mats [17]. Although such totally green natural fibre parts display mechanical properties comparable to conventional composites manufactured with synthetic glue, for some more demanding applications the performance of binder-less *Typha*-boards may not be sufficient.

In order to enhance the technological properties, in the present study small amounts of an additional bio-based binder resin were used to prepare novel, totally green *Typha* based composites. As the binder resin, a mixture of an epoxidized linseed oil with a tall-oil based polyamide curing agent was used [18]. The simplified reaction scheme in Scheme 1 depicts representative components of the original bio-renewable starting materials linseed oil (a) and tall oil (b) and the general chemistry leading to the cross-linked bio-based binder material used in the present study (c). Linseed oil is rich in triglycerides comprising oleic acid, linoleic acid and α-linolenic acid. The unsaturated C=C double bonds can readily be converted into oxirane functionalities ultimately yielding bio-based epoxy resins [19–22] or upon further transformation non-isocyanate based polyurethane resins [23] or photocrosslinkable coatings [24,25].

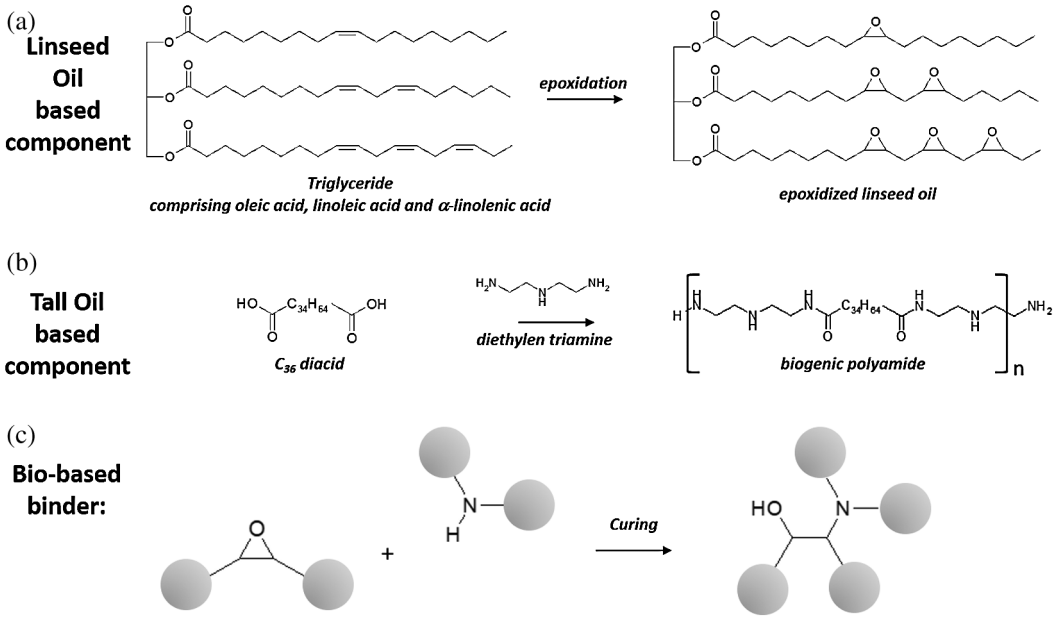

Scheme 1: (a) Typical component of linseed oil and simplified reaction scheme for conversion to the epoxy component of the used bio-binder system. (b) Biogenic polyamide resulting from reaction of a C_{36} fatty acid derived from tall oil with diethylene triamine. (c) Simplified initial curing reaction in the employed bio-binder resin between epoxidized linseed oil and tall oil-based polyamide

Tall-oil is derived as a by-product from the Kraft pulping process and has a typical composition of 38–53 wt.% fatty acids, 38–53 wt.% rosin acids, and 6.5–20 wt.% unsaponified (neutral) compounds [18,26,27]. The polyamide used in this study was derived from a dimeric C_{36} fatty acid obtained from the tall oil which had been reacted with diethylene triamine [18] yielding the basic structural element depicted in Scheme 1(b). This polyamide carried reactive amine groups and was used to cross-link the epoxidized linseed oil (Scheme 1(a)). The simplified initial curing reaction step is depicted in Scheme 1(c).

The combination of *Typha latifolia* fibrous material with the epoxidized linseed-oil/tall oil-based binder yielded totally green composite materials solely based on renewable resources. Their technological properties were compared to the properties of binder-less *Typha* composites. The curing conditions for composite pressing were optimized using differential scanning (DSC) analysis of the bio-binder and modelling the thermochemical data with iso-conversional kinetic analysis.

2 Theory of Iso-Conversional Kinetic Analysis

Iso-conversional kinetic analysis [28] has been widely applied for studying and optimizing the curing behavior of many different chemical binder systems such as melamine formaldehyde [29], phenol-formaldehyde [30], lignin-based [31,32], epoxy-based [33,34], and other resins like epoxized linseed oil/anhydride hardener systems [35] or complex powder coatings [36]. Iso-conversional kinetic analysis allows defining process windows and predicting technological property profiles of the finished parts based on curing profiles of the binder system as shown for laminate surface finishes [37] or powder coated surfaces [38].

The mathematical basis for describing the effect of temperature on the rate of a chemical process is the fundamental rate equation originally established by Arrhenius [39]. The Arrhenius approach uses three kinetic parameters to model the progress of a chemical reaction: the pre-exponential factor, A, the activation energy, E_a, and the reaction model, $f(\alpha)$. Therefore, the classical kinetic analysis of rate data requires information on the reaction mechanism (which is the "reaction model" $f(\alpha)$): it is said to be model-dependent. However, with multistep-reactions involving a multitude of chemical equilibria the reaction mechanism is rarely known quantitatively [40]. Examples for such reactions are, for instance, thermal degradation processes, the cross-linking of thermosetting resins in general or, more specifically, the curing of our bio-based binder resin.

In such cases, model-dependent approaches are often prone to yield inaccurate results and, as an alternative, model-free kinetic (MFK) or so-called "iso-conversional" methods have been developed [41]. These approaches are based on the iso-conversional principle, which states that the apparent activation energy at a particular degree of cure, α, does not depend on the applied temperature gradient. Iso-conversional methods are classified in either differential or integral methods. In the present study, we use the integral approach introduced and further developed to an advanced form by Vyazovkin [42] (abbreviated in the following by "VA") to model the dependence of the effective activation energy on the degree of cure, $E_a(\alpha)$, for the resin mixture of epoxidized linseed oil with tall-oil based polyamide.

All integral methods are based on the iso-conversional principle implying that for any heating rate β the integral form of the reaction model g (α) is constant according to Eq. (1).

$$g(\alpha) = \int_0^{\alpha} \frac{d\alpha}{f(\alpha)} = \frac{A}{\beta} \int_0^{T} \exp\left(\frac{-E(\alpha)}{RT}\right) dT = \frac{A}{\beta} I[E(\alpha), T] \tag{1}$$

In the VA-approach E_α is determined by iteration and minimizing by Eq. (2):

$$\sum_{i=1}^{n} \sum_{j\neq 1}^{n} \frac{I[E_a(\alpha), T]_i \beta_j}{I[E_a(\alpha), T]_j \beta_i} \tag{2}$$

With the calculated E(α)-curves the time (t_α) required for a certain degree of cure α of the bio-based resin at an arbitrary isothermal temperature (T_0) can be estimated [41] using the Eq. (3)

$$t_\alpha = \frac{\int_0^T \exp\left(\frac{-E_a(\alpha)}{RT}\right) dT}{\beta \exp\left(\frac{-E_a(\alpha)}{RT_0}\right)} \tag{3}$$

With the knowledge about the cure kinetics always the time for arbitrary temperatures (in a hot press but also in a tempering oven) can be calculated which in turn can be used to derive curing process conditions that yield completely cured resin.

3 Materials and Methods

3.1 Chemicals

The resin components used in this study were a commercial epoxidized linseed oil, Dehysol B 315 (Cognis GmbH), and a commercial tall-oil based polyamide, Unirez 2125 (Arizona Chemical). For impregnation and for DSC analysis both components were mixed together in the proportion of 1:1.

3.2 Vegetable Fibres

For the composites the broad-leaved cattail species *Typha latifolia* was used. Staple fibres of *Typha latifolia* were delivered from Naporo Klima Dämmstoff GmbH (Moosdorf, Austria).

3.3 Thermochemical Analysis by Differential Scanning Calorimetry and Iso-Conversional Kinetic Analysis

The cross-linking degree, α, of the bio-resin was derived from dynamic DSC traces was measured with the 822e differential scanning calorimeter by Mettler-Toledo (Greifensee, Switzerland). The exothermal enthalpy changes were recorded and integrated over the reaction time (from time t_{start} to t_{end} and from temperature T_{start} to T_{end}, respectively) during curing which lead to the total cure enthalpy, ΔH_{t_end}. To obtain sample-weight independent values, the enthalpy integral was normalized to the sample weight (H in J g^{-1}). From H of each DSC trace the degree of cure α was calculated as a function of time (t). α(t) was calculated as the ratio between the partly integrated curing enthalpy from time t_{start} to t (ΔH_t) and the total curing enthalpy ΔH_{t_end} using Eq. (4).

$$\alpha(t) = \Delta H_t / \Delta H_{t\_end} \tag{4}$$

The software package STAR 8.10. (Mettler Toledo, Greifensee, Switzerland) was used for the calculation of all the α (t)-curves. For further kinetic analysis one iso-conversional kinetic analysis (ICKA) technique, the approach of Vyazovkin in its advanced form (VA) was used. Three α (t)-curves, one for each heating rate (5, 7.5 and 10°C min^{-1}), were used to calculate the apparent activation energy (E) as function of the degree of cure (α) with the VA-approach. For the minimizing process in the VA-approach a software program was written by using the mathematical software package MATLAB Version 7.7. The integral (I) in Eq. (2) was solved by the function called "expint," an implementation of the direct integration method [43]. The numerical minimization of the Eq. (2) was solved by the function called "fminunc."

3.4 Manufacturing of Composites

The manufacturing of fibre mats composed of *Typha* fibres followed the procedure described in [17] and involved the opening of *Typha* fibre bundles on a carding machine followed by layering the fibres to a fibre felt with the SPIKE technology, which is a combination of traditional air-laid and carding technology [44]. Thereafter, fibre mats with an area weight of 1.200 g/m² were produced by needle-punching of the fibre felts. Thereafter, some of the fibre mats remained binder-less, without drying others were impregnated with the bio-based resin mixture to obtain a composite with a binder content of 10 wt-% in the final composite.

Both binder-less and impregnated mats were compression moulded into panels at a constant pressing temperature of 160°C and a constant pressure of 80 bar. Because of the manufacturing process the fibre mats as well as the moulded composites have anisotropic mechanical properties. Hence, flexural strength measurements were always performed on test specimens, where two *Typha* fibre mats had been pressed crosswise into a laminate with respect to the production direction. While the first *Typha* fibre mat had its main fibre-axis oriented in parallel to direction of the production line, the second fibre mat was arranged perpendicular to this direction to account for the anisotropy. The binder-less *Typha* mats and the *Typha* mats impregnated with the bio-resin were pressed with three different pressing times, t_1 = 60 min, t_2 = 120 min, and t_3 = 180 min. The curing procedure for the bio-resin containing *Typha* panels was complemented by a post-curing phase at 100°C. The duration of post-curing was determined by iso-conversional analysis of the curing degree of the partially cured bio-resin upon DSC analysis of liquid resin samples.

The morphology of the *Typha* fibre with and without binder was observed under a Phenom Pro X SEM (Phenom-World, Eindhoven, Netherlands) with an acceleration voltage of 15 kV. The fibre and the composites were deposited on a carbon-coated grid, air dried and sputter coated with gold in a SC7620 mini sputter coater (Quorum Technologies Ltd., Kent, UK).

3.5 Technological Testing of Composites Properties

The thickness of the composite was measured by using vernier caliper and the density was calculated from the measured dimensions and weight.

As technological properties the flexural strength, the flexural modulus of elasticity (MOE) and the water absorption of each moulded composite were measured. The flexural properties were measured according to the standard DIN EN 310 and the water absorption according to the standard DIN 52351.

4 Results and Discussion

4.1 Characterization of Curing Behavior of the Bio-Resin

To derive a quantitative model allowing to calculate the conditions required for a completely cured resin at an arbitrary temperature, as a first step, the cure kinetics of the bio-based resin was analyzed. For the kinetic analysis of resin cure, differential scanning calorimetry (DSC) in combination with the iso-conversional kinetic analysis (ICKA) method of Vyazovkin (VA) was used.

The DSC thermograms at three heating rates (5, 7.5, and 10°C min^{-1}) from 25°C to 300°C are shown in Fig. 1. Based on the thermograms the E (α)-curves were calculated with the VA-approach which in turn was used to derive theoretical curing isotherms (Fig. 2) using Eq. (3).

To validate the ICKA, partially cured resin mixtures were prepared applying a heat treatment that yielded different defined cure degrees α as predicted by the VA-approach. Using the ICKA-model based on theoretical isotherms, for a reaction temperature of 180°C and different targeted cross-linking degrees (10, 20, 30, 40, 50, 60, 70, 80, 90, and 94%) the experimentally required corresponding reaction times were calculated by using Eq. (3). Samples of resin mixtures were pressed in a hot press at a plate temperature of T = 180°C for the different durations of time to obtain specified cure degrees α. The

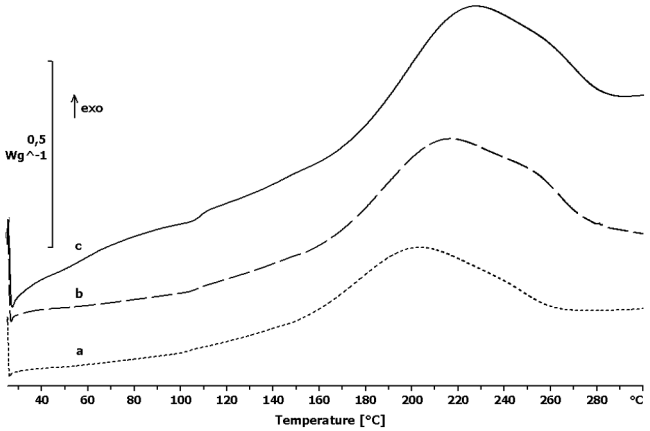

Figure 1: DSC traces of bio-resin at different heating rates. (a) 5, (b) 7.5 (c) and 10°C min^{-1}

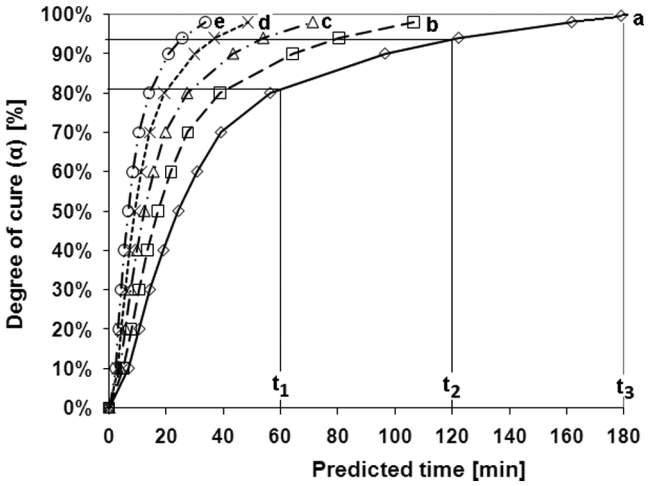

Figure 2: Degree of cure as function of time predicted by kinetic model, calculated for five temperatures. (a) 160, (b) 170, (c) 180, (d) 190 and (e) 200°C—Matching of three different press times, t_1 = 60 min, t_2 = 120 min, and t_3 = 180 min at press temperature of 160°C (a) with degree of cure for t_1 = 81%, t_2 = 94%, and t_3 = 100%

partially cured samples were then used for validating the kinetic model. For this, they were analysed by DSC at a heating rate of 10°C min^{-1} and the cure degree α was calculated according to Eq. (4). The validation plot in Fig. 3 shows the measured degree of partially cured resin (points) in comparison with the predicted degree of cure (solid line). The measured cure degree was slightly higher than predicted (mean difference = +3.5%).

4.2 Determination of the Ideal Curing Protocol for the Bio-Resin

The theoretical curing isotherms derived for 5 arbitrary temperatures are shown in Fig. 2. For the pressed *Typha* fibre mats containing 10% bio-resin, that were prepared at the three pressing times t_1 = 60 min, t_2 = 120 min, and t_3 = 180 min at the pressing temperature of 160°C the curing degree was calculated using the curing isotherm data at 160°C. According to the MFK model, a pressing time of 60 minutes resulted in a curing degree of 81%, whereas a pressing time of 120 minutes yielded a curing degree of 94%. Only the pressing time 180 minutes led to the maximum curing degree of 100%.

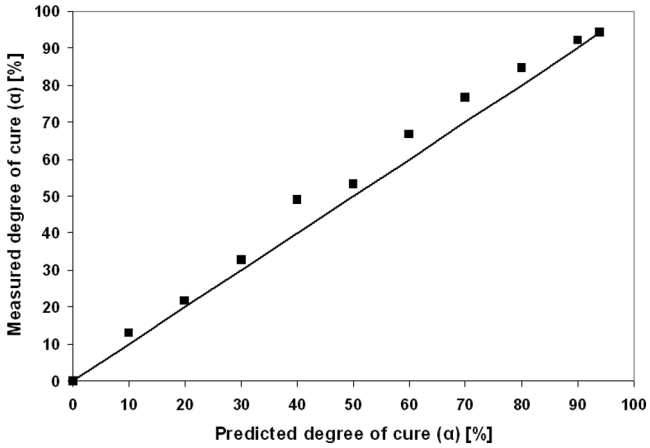

Figure 3: Validation plot of the kinetic model for resin curing. The individual points indicated the measured degree of cure and solid line indicates the degree of cure predicted by the model

The results of the thermochemical analysis of the bio-based resin showed that for the pressing temperature of 160°C a pressing time of approximately 180 min was sufficient and necessary for complete cure of the bio-resin. In contrast, after the shorter pressing times t_1 and t_2, the panels cannot be expected to be completely cured. By an additional subsequent post-curing step at a temperature of 100°C in an oven, for both panels, however, a curing degree of 100% was brought about. The required residence time for post-curing at 100°C was calculated for both panels from the corresponding model curing isotherms at this temperature obtained from the iso-conversional kinetic analysis.

With the theoretical curing isotherm for the tempering oven temperature of 100°C the tempering time to reach 100% degree of resins cure was calculated: The additional post-curing times were 42 hours for the panel with press time t_1 and 13 hours for the panel with press time t_2. Since the resin contained in the panel with press time 180 min was completely cured after the initial pressing step, no additional post-curing was performed with this panel.

4.3 Morphology of the Composite Material

Fig. 4 shows a typical *Typha* fibre mat before pressing (a) as well as binder-less (b) and bio-binder containing (c) *Typha* fibre composites after pressing.

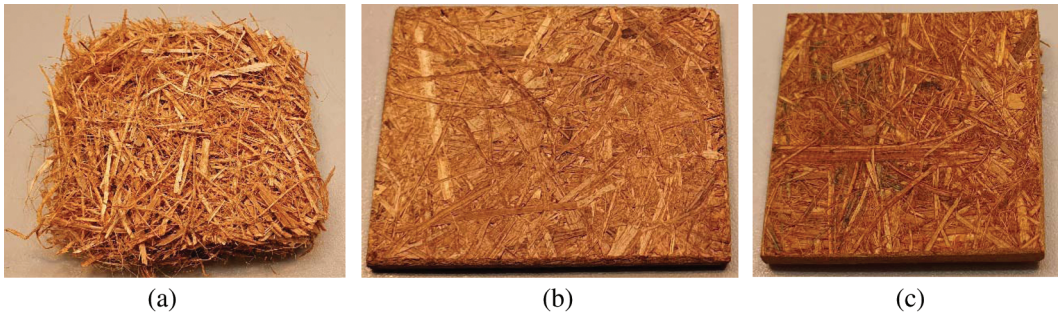

(a) (b) (c)

Figure 4: *Typha* fibre mat (a) and after pressing without (b) and with (c) bio-binder

The morphology of the fibre and the reinforced composites was analysed using scanning electron microscopy. The cross-section of the *Typha* fibre is shown in Figs. 5a and 5b. The micrographs show the

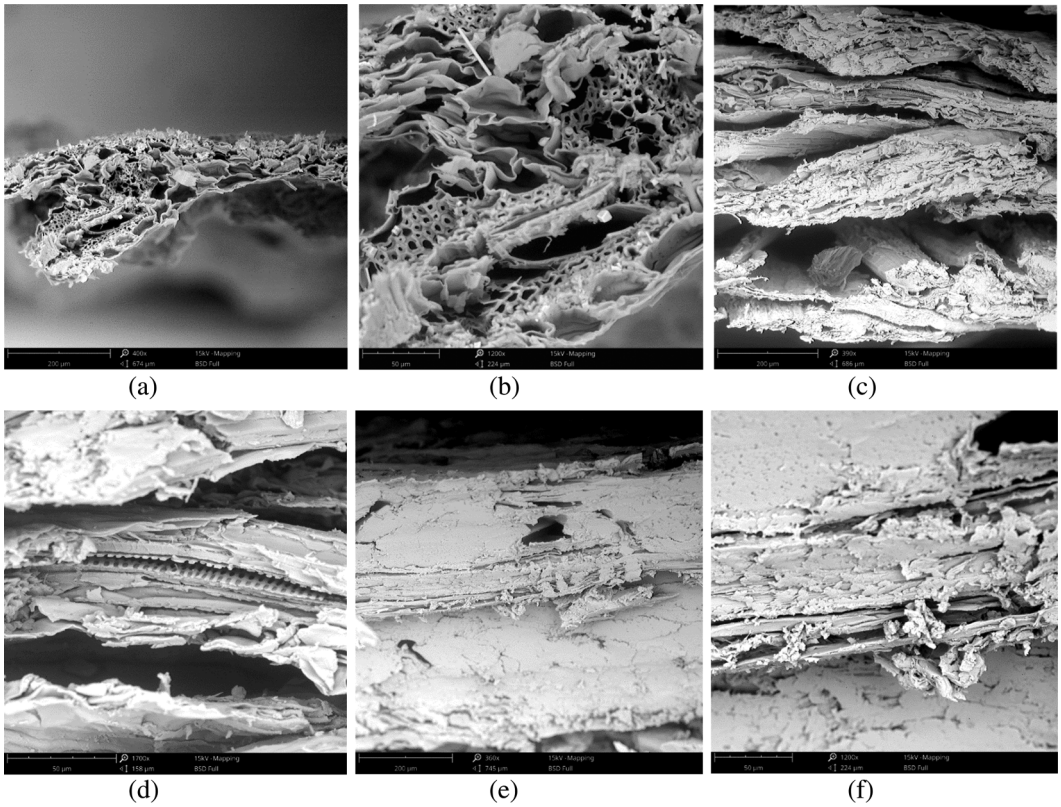

Figure 5: Cross-section of the *Typha* binder (a) and magnified image (b), fractured surface of the *Typha* self-reinforced composite without binder (c) and magnified image (d), and fractured surface of the *Typha* composite with binder (e) and magnified image (f)

hollow lumen structure of the *Typha* fibre at different magnification factors. The fractured surface of the composites with and without binder is shown in Figs. 5c–5f. One can see the accumulation of the binder inside the composites and the matrix wetted on the fibre surface. The 10 wt.% is not well enough to completely bind the whole reinforcement because some voids were observed in between the reinforcements.

4.4 Technological Properties of Typha Composites with Bio-Resin

With the aim to meet higher demands in technological properties an ecologically harmless, bio-based resin was added to *Typha* composites. Just as binder-less reference *Typha* mats, the *Typha* mats impregnated with the bio-based resin were pressed at a constant press temperature with increasing press times to panels with different densities. The results of both measured flexural properties of these panels are presented in Figs. 6 and 7 respectively.

Both flexural properties, the flexural MOE (Fig. 6) and the flexural strength (Fig. 7), depended on the density of the bioresin-bonded *Typha* panels, regardless of the chosen pressing time. The higher the density of the panel, the higher are the values for the flexural properties. The flexural MOE increases linearly and the flexural strength increases exponentially as the panel density increases (see solid regression lines in Figs. 6 and 7). The dependence of water sorption properties on the density of bioresin-bonded *Typha* panels was indirectly proportional to panel density. The water absorption of panels decreased linearly as the panel density increased regardless of the chosen pressing time. Hence, for all panels a single linear regression model for water absorption as a function of panel density was calculated (see solid line of linear regression in Fig. 8).

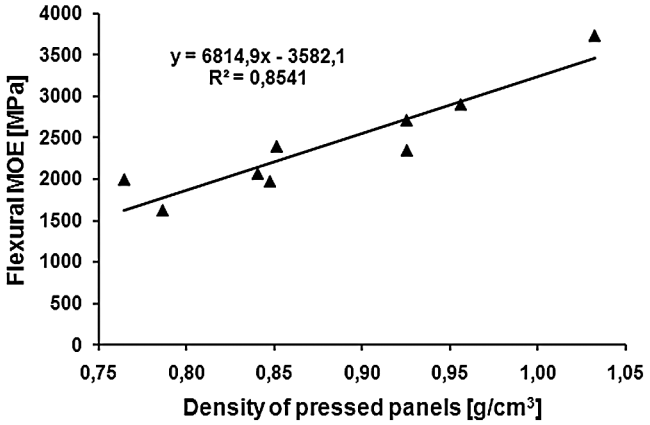

Figure 6: Flexural MOE of *Typha* panels with 10 wt-% bio-based resin and with different densities (triangles) and linear regression of flexural MOE on density (solid line)

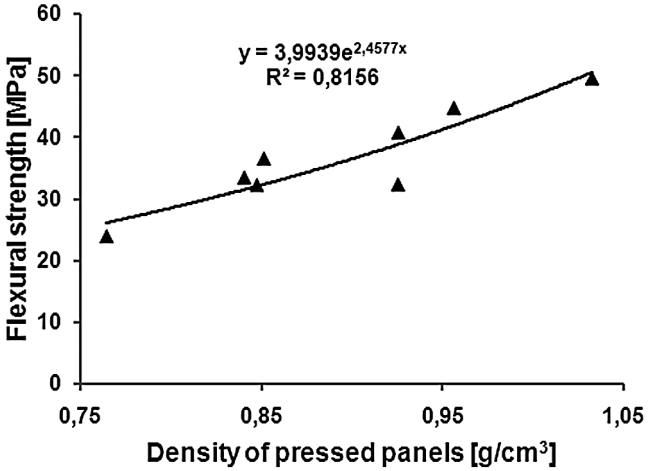

Figure 7: Flexural strength of *Typha* panels with 10 wt-% bio-based resin and with different densities (triangles) and linear regression of flexural strength on density (solid line)

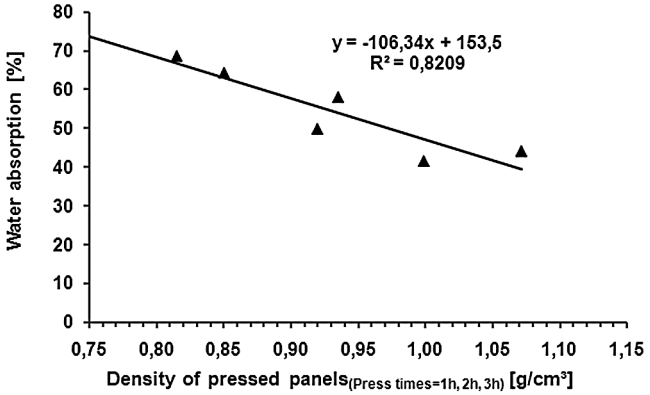

Figure 8: Water absorption of all *Typha* panels with 10 wt-% bio-based resin (triangles) and linear regression of water absorption on density (solid line)

Using the regression function given in Fig. 8, the water absorption can be calculated as a function of pressing time for an arbitrary panel density and be normalized to a density of 1 g/cm³. Such density normalized water absorption is constant at a mean value of about 54% and a standard deviation of about 11% as the pressing time increases (mean value as triangles with standard deviation in Fig. 9).

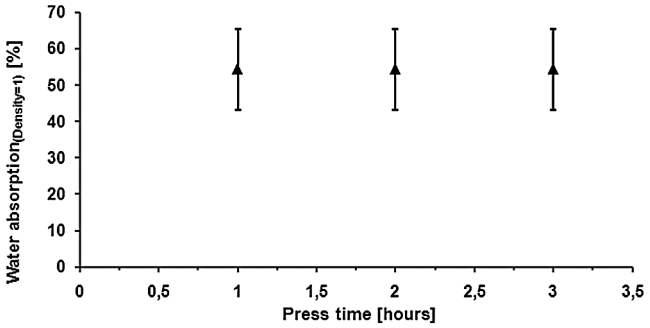

Figure 9: Water absorption of *Typha* panels with 10 wt-% bio-based resin calculated for panel density = 1 g/cm³ using regression equation in Fig. 8 for different press times (triangles)

4.5 Comparison of Technological Properties of Typha Composites with and without Bio-Resin

For comparison the flexural properties of binder-less *Typha* panels and *Typha* panels with 10 wt-% bio-based resin are shown in Figs. 10 and 11 respectively. *Typha* panels made using bio-based resins with densities lower than 1 g/cm³ had higher flexural MOE than the binder-less *Typha* panels with the same low densities. In contrast, when the panel density exceeded 1 g/cm³, the binder-less *Typha* panels had higher flexural MOE than the panels with bio-resin (see Fig. 10). On the other hand, the flexural strength of panels with additional bio-based resin was always higher than the flexural strength of binder-less panels regardless of the panel density (see Fig. 11).

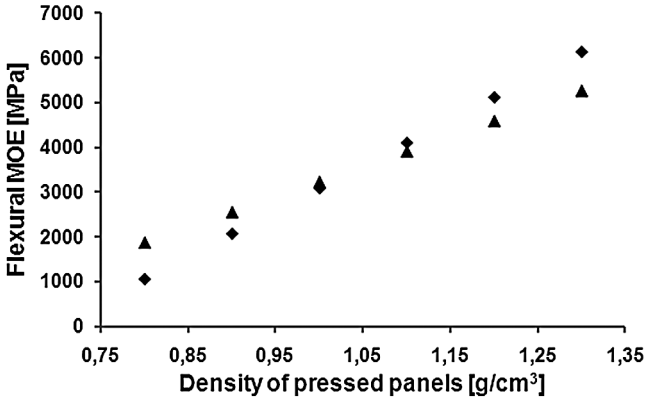

Figure 10: Flexural MOE with different panel densities—comparison of binder-less *Typha* panels (diamonds) with *Typha* panels with 10 wt-% bio-based resin (triangles)

These results can be explained as follows: In optimal fibre reinforced polymers the reinforcement fibres increase the mechanical strength of the polymer while the polymer has the function of a binder matrix that holds the fibres together in a fixed position and transmits mechanical forces between the fibres. If the amount of binder is low, the risk of areas where fibres are not impregnated is increased. In that case, the transmission of mechanical forces is disturbed and the mechanical performance is lower than theoretically possible. In the

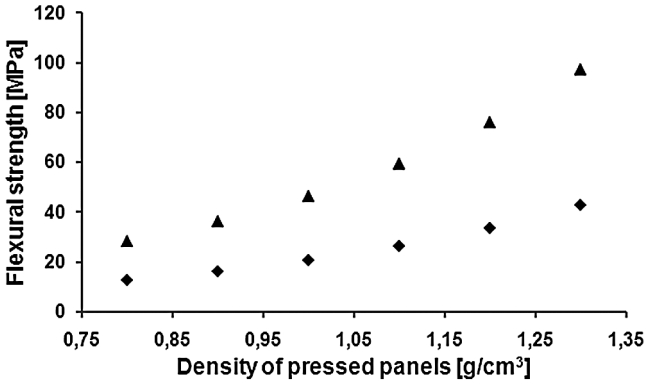

Figure 11: Flexural strength for different panel densities—comparison of binder-less *Typha* panels (diamonds) with *Typha* panels with 10 wt-% bio-based resin (triangles)

pressed binder-less panels the natural substances present in *Typha* can act as binder. However, the content of natural binder is rather low and not sufficient to impregnate the fibres completely. This explains why the flexural strength of panels with additional 10 wt.-% of bio-based resin was always higher than the flexural strength of the binder-less panels (see Fig. 11). On the other hand, both flexural MOE (Fig. 10) and flexural strength (Fig. 11) could be increased by pressing the fibers with a given amount of binder to panels at higher pressure forces, because due to the higher compaction more fibres could be brought into contact with the existing binder content. Furthermore, the curves of flexural MOE in Fig. 10 show that when the compaction was high enough the issue of low binder content was compensated. Hence, only in the case of high pressure forces the higher content of reinforcing fibres in binder-less panels resulted in the expected higher flexural MOE in comparison to the panels with 90/10 wt/wt fibre/binder proportions.

Whereas the water absorption of binder-less *Typha* panels depends on both process parameters, the press time and the panel density, the water absorption of *Typha* panels with bio-based resin does not depend on the press time and only slightly on the density (Fig. 12). The water absorption was significantly improved by the addition of the bio-based resin and this improvement is much higher if the density of the panel is low.

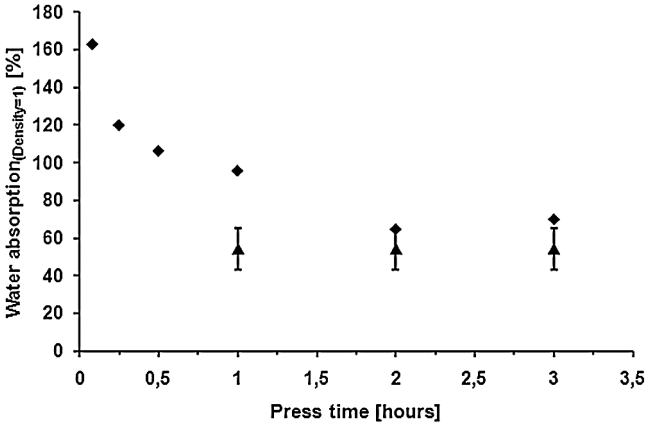

Figure 12: Water absorption normalized to panel density = 1 g/cm³ for different press times—comparison of binder-less *Typha* panels (diamonds) with *Typha* panels with 10 wt-% bio-based resin (triangles)

5 Conclusion

In this contribution, we describe the technological properties of composites made from vegetable fibres from *Typha* sp. as reinforcement in "green" composites. *Typha* composites were tested binder-less, where only the naturally occurring constituents of cattails acted as binder. The flexural MOE, the flexural strength and the water absorption of binder-less *Typha* panels were measured and the influence of pressing time and panel density on these properties was investigated. The best properties were achieved for panels with high density regardless of the chosen press time. With the aim to meet higher demands in technological properties an ecologically harmless, bio-based resin consisting of a mixture of an epoxidized linseed oil and tall-oil based polyamide was added to *Typha* composites in a small proportion of 10 wt-%. The cure kinetics of the resin was analysed by differential scanning calorimetry (DSC) in combination with the isoconversional kinetic analysis (ICKA) method of Vyazovkin (VA) to calculate the time for arbitrary temperatures (in a hot press but also in a tempering oven) leading to a completely cured resin. For comparison the *Typha* composites with binder were pressed at same press times as the binder-less *Typha* composites were pressed but with additional annealing in a tempering oven to guarantee completely cured resin for all panels. Cattails for binder-less composites have high potential for novel "green" composites and by adding small amounts of the bio-based resin the flexural strength and the water absorption were improved significantly.

Acknowledgement: This project was made possible by funding and support from the Austrian Research Promotion Agency (FFG). The authors would like to thank Dr. Matea Perić (Kompetenzzentrum Holz GmbH) for the SEM measurements.

Funding Statement: This project was made possible by funding and support from the Austrian Research Promotion Agency (FFG).

Conflicts of Interest: The authors declare that they have no conflicts of interest to report regarding the present study.

References

1. Müssig, J. (2010). *Industrial applications of natural fibres. Structure, properties and technical applications*. Chichester, UK: Wiley.
2. Saheb, D. N., Jog, J. P. (1999). Natural fibre polymer composites: a review. *Advances in Polymer Technology, 18 (4),* 351–363. DOI 10.1002/(SICI)1098-2329(199924)18:4<351::AID-ADV6>3.0.CO;2-X.
3. Hejna, M., Moscatelli, A., Stroppa, N., Onelli, E., Pilu, S. et al. (2020). Bioaccumulation of heavy metals from wastewater through a *Typha latifolia* and *Thelypteris palustris* phytoremediation system. *Chemosphere, 241,* 125018. DOI 10.1016/j.chemosphere.2019.125018.
4. Batool, A. (2019). Metal accumulation from leachate by polyculture in crushed brick and steel slag using pilot-scale constructed wetland in the climate of Pakistan. *Environmental Science and Pollution Research, 26(30),* 31508–31521. DOI 10.1007/s11356-019-06211-w.
5. Papadopoulos, N., Zalidis, G. (2019). The use of Typha Latifolia L. in constructed Wetland microcosms for the remediation of herbicide terbuthylazine. *Environmental Processes, 6(4),* 985–1003. DOI 10.1007/s40710-019-00398-3.
6. Yang, Y., Shen, Q. (2019). Phytoremediation of cadmium-contaminated wetland soil with *Typha latifolia* L. and the underlying mechanisms involved in the heavy-metal uptake and removal. *Environmental Science and Pollution Research, 27(5),* 4905–4916. DOI 10.1007/s11356-019-07256-7 (in press).
7. Parzych, A., Sobisz, Z. (2018). The accumulation of trace elements in organs of *Typha latifolia* L. in rural pond ecosystems with varying degrees of pollution. *Ecohydrology & Hydrobiology, 18(3),* 297–306. DOI 10.1016/j.ecohyd.2018.06.003.

8. Ciuca, I., Stanescu, M. M., Bolcu, D. (2018). A study on the mechanical properties of some green composites. *Environmental Engineering and Management Journal, 17(12),* 2991–2998. DOI 10.30638/eemj.2018.299.
9. Daud, Y. M., Yee, T. G., Adnan, S. A., Taidi, H. A. (2018). Tensile and thermal degradation properties of poly (lactic acid)/*Typha Latifolia* bio-composites. *AIP Conference Proceedings*, 020048, 2030.
10. Balaed, K., Noriman, N. Z., Dahham, O. S., Sam, S. T., Hamzah, R. et al. (2016). Characterization and properties of low-linear-density polyethylene/Typha latifolia composites. *International Journal of Polymer Analysis and Characterization, 21(7),* 590–598. DOI 10.1080/1023666X.2016.1183336.
11. Bajwa, D. S., Sitz, E. D., Bajwa, S. G., Barnick, A. R. (2015). Evaluation of cattail (Typha spp.) for manufacturing composite panels. *Industrial Crops and Products, 75,* 195–199. DOI 10.1016/j.indcrop.2015.06.029.
12. Ibrahim, M., Jalil, J. A., Mahamud, S. N. S., Daud, Y. M., Husseinsyah, S. et al. (2013). Tensile and morphology properties of polylactic acid/treated *Typha latifolia* composites. *Key Engineering Materials, 594–595,* 775–779. DOI 10.4028/www.scientific.net/KEM.594-595.775.
13. Ramanaiah, K., Prasad, A. V., Ratna, A., V., Hema Chandra Reddy, K. (2011). Mechanical properties and thermal conductivity of typha angustifolia natural fiber-reinforced polyester composites. *International Journal of Polymer Analysis and Characterization, 16(7),* 496–503. DOI 10.1080/1023666X.2011.598528.
14. Sana, R., Foued, K., Yosser, B. M., Mounir, J., Slah, M. et al. (2015). flexural properties of typha natural fiber-reinforced polyester composites. *Fibers and Polymers, 16(11),* 2451–2457. DOI 10.1007/s12221-015-5306-x.
15. McManus, H. A., Seago, J. L. Jr., Marsh, L. C. (2002). Epifluorescent and histochemical aspects of shoot anatomy of *Typha latifolia* L., Typha angustifolia L. and Typha glauca Godr. *Annals of Botany, 90,* 489–493.
16. Seago, J. L., Jr, Peterso, C. A., Enstone, D. E., Scholey, C. (1999). Development of the endodermis and hypodermis of *Typha glauca* Godr and Typha angustifolia L. roots. *Canadian Journal of Botany, 77,* 122–134.
17. Wuzella, G., Mahendran, A. R., Bätge, T., Jury, S., Kandelbauer, A. (2011). Novel, binder-free fiber reinforced composites based on a renewable resource from the reed-like plant *Typha* sp. *Industrial Crops and Products, 33(3),* 683–689. DOI 10.1016/j.indcrop.2011.01.008.
18. Dubowik, D. A., Walker, F. H., Starner, W. E. (1999). Novel curing agent technology for high solids epoxy coatings. *International Waterborne, High Solids, and Powder Coatings Symposium*. *New Orleans*.
19. Miyagawa, H., Mohanty, A. K., Misra, M., Drzal, L. T. (2004). Thermo-physical and impact properties of epoxy containing epoxidized linseed oil. Part 1. *Macromolecular Materials and Engineering, 289(7),* 629–635. DOI 10.1002/mame.200400004.
20. Miyagawa, H., Mohanty, A. K., Misra, M., Drzal, L. T. (2004). Thermo-physical and impact properties of epoxy containing epoxidized linseed oil. Part 2. *Macromolecular Materials and Engineering, 289(7),* 636–641. DOI 10.1002/mame.200400003.
21. Pin, J. M., Sbirrazzuoli, N., Mija, A. (2015). From epoxidized linseed oil to bioresin: an overall approach of epoxy/anhydride cross-linking. *ChemSusChem, 8(7),* 1232–1243. DOI 10.1002/cssc.201403262.
22. Mahendran, A. R., Aust, N., Wuzella, G., Kandelbauer, A. (2012). Synthesis and characterization of a bio-based resin from linseed oil. *Macromolecular Symposia, 311(1),* 18–27. DOI 10.1002/masy.201000134.
23. Mahendran, A. R., Aust, N., Wuzella, G., Müller, U., Kandelbauer, A. (2012). Bio-based non-isocyanate urethane derived from plant oil. *Journal of Polymers and the Environment, 20(4),* 926–931. DOI 10.1007/s10924-012-0491-9.
24. Wuzella, G., Mahendran, A. R., Müller, U., Kandelbauer, A., Teischinger, A. (2012). Photocrosslinking of an acrylated epoxidized linseed oil: kinetics and its application for optimized wood coatings. *Journal of Polymers and the Environment, 20(4),* 1063–1074. DOI 10.1007/s10924-012-0511-9.
25. Mahendran, A. R., Wuzella, G., Aust, N., Kandelbauer, A., Müller, U. (2012). Photocrosslinkable modified vegetable oil based resin for wood surface coating application. *Progress in Organic Coatings, 74(4),* 697–704. DOI 10.1016/j.porgcoat.2011.09.027.
26. de Kruijff, G. H. M., Goschler, T., Derwich, L., Beiser, N., Türk, O. M. et al. (2019). Biobased epoxy resin by electrochemical modification of tall oil fatty acids. *ACS Sustainable Chemistry & Engineering, 7(12),* 10855–10864. DOI 10.1021/acssuschemeng.9b01714.

27. Zhang, J., Nunez, A., Strahan, G. D., Ashby, R., Huang, K. et al. (2020). An advanced process for producing structurally selective dimer acids to meet new industrial uses. *Industrial Crops and Products, 146,* 112132. DOI 10.1016/j.indcrop.2020.112132.
28. Vyazovkin, S. (2015). *Isoconversional kinetics of thermally stimulated processes*. Heidelberg, Berlin; New York: Springer.
29. Kandelbauer, A., Wuzella, G., Mahendran, A., Taudes, I., Widsten, P. (2009). Model-free kinetic analysis of melamine-formaldehyde resin cure. *Chemical Engineering Journal, 152(2–3),* 556–565. DOI 10.1016/j.cej.2009.05.027.
30. Tejado, A., Kortaberria, G., Labidi, J., Echeverria, J. M., Mondragon, I. (2008). Isoconversional kinetic analysis of novolac-type lignophenolic resins cure. *Thermochimica Acta, 471(1–2),* 80–85. DOI 10.1016/j.tca.2008.03.005.
31. Ammar, M., Khiari, R., Belgacem, M. N., Elaloui, E. (2015). Gelation and isoconversional kinetic analysis of synthesis of lignin-resorcinol-glyoxal resin curing. *Iranian Polymer Journal, 24(11),* 919–925. DOI 10.1007/s13726-015-0380-x.
32. Mahendran, A. R., Wuzella, G., Kandelbauer, A. (2010). Thermal characterization of kraft lignin phenol-formaldehyde resin for paper impregnation. *Journal of Adhesion Science and Technology, 24(8),* 1553–1565. DOI 10.1163/016942410X500936.
33. Granado, L., Kempa, S., Gregoriades, L. J., Brüning, F., Genix, A. et al. (2018). Kinetic regimes in the curing process of epoxy-phenol composites. *Thermochimica Acta, 667,* 185–192. DOI 10.1016/j.tca.2018.07.019.
34. Fan, M., Liu, J., Li, X., Cheng, J., Zhang, J. (2013). Curing behaviors and properties of an extrinsic toughened epoxy/anhydride system and an intrinsic toughened epoxy/anhydride system. *Thermochimica Acta, 554,* 39–47. DOI 10.1016/j.tca.2012.12.007.
35. Mahendran, A. R., Wuzella, G., Kandelbauer, A., Aust, N. (2012). Thermal cure kinetics of epoxidized linseed oil with anhydride hardener. *Journal of Thermal Analysis and Calorimetry, 107(3),* 989–998. DOI 10.1007/s10973-011-1585-7.
36. Wuzella, G., Kandelbauer, A., Mahendran, A. R., Teischinger, A. (2011). Thermochemical and isoconversional kinetic analysis of a polyester–epoxy hybrid powder coating resin for wood-based panel finishing. *Progress in Organic Coatings, 70(4),* 186–191. DOI 10.1016/j.porgcoat.2010.09.023.
37. Kandelbauer, A., Wuzella, G., Mahendran, A., Taudes, I., Widsten, P. (2009). Using isoconversional kinetic analysis of liquid melamine formaldehyde resin curing to predict laminate surface properties. *Journal of Applied Polymer Science, 113(4),* 2649–2660. DOI 10.1002/app.30294.
38. Wuzella, G., Kandelbauer, A., Mahendran, A. R., Müller, U., Teischinger, A. (2014). Influence of thermo-analytical and rheological properties of an epoxy powder coating resin on the quality of coatings on medium density fibreboards (MDF) using in-mould technology. *Progress in Organic Coatings, 77(10),* 1539–1546. DOI 10.1016/j.porgcoat.2013.10.016.
39. Galwey, A. K., Brown, M. E. (1998). Chapter 3. Kinetic background to thermal analysis and calorimetry. In Brown, M. E. (eds.) *Handbook of Thermal Analysis and Calorimetry.* vol. 1. pp. 147–224. Amsterdam, The Netherlands: Principles and Practice, Elsevier Science B.V.
40. Ghaemy, M., Riahy, M. H. (1996). Kinetics of anhydride and polyamide curing of bisphenol a-based diglycidyl ether using DSC. *European Polymer Journal, 32(10),* 1207–1212. DOI 10.1016/S0014-3057(96)00066-3.
41. Vyazovkin, S., Sbirrazzuoli, N. (2006). Isoconversional kinetic analysis of thermally stimulated process in polymers. *Macromolecular Rapid Communications, 27(18),* 1515–1532. DOI 10.1002/marc.200600404.
42. Vyazovkin, S. (2001). Modification of the integral isoconversional method to account for variation in the activation energy. *Journal of Computational Chemistry, 22(2),* 178–183. DOI 10.1002/1096-987X(20010130)22:2<178::AID-JCC5>3.0.CO;2-#.
43. Gautschi, W., Cahill, W. F. (1965). Chapter 5. Exponential integral and related functions. In Abramowitz, M., Stegun, I. A. (eds.) *Handbook of Mathematical Functions*. pp. 228–254. New York: Dover Publications Inc.
44. Andersen, C. (2005). Fibre distribution device for dry forming a fibrous product. WO/2005/044529 A1 (PCT/DK2004/000732).